Pink NIR pigment based on Cr doped $SrSnO_3$: Preparation and characterization

Žaneta Dohnalová, Petra Šulcová, Petr Bělina

Department of Inorganic Technology, Faculty of Chemical Technology, University of Pardubice, Studentská 573, 532 10 Pardubice, Czech Republic.

E-mail: zaneta.dohnalova@.upce.cz

Abstract

Perovskite pigments with $SrCr_xSn_{1-x}O_{3-\delta}$ (x = 0.025, 0.05, 0.1, 0.2, 0.3) composition were prepared by a solid-state reaction, suspension mixing of materials, and mechanochemical activation of initial reagents with calcination at high temperature. Results of thermal analysis show the effectivity of mechanochemical activation of reaction mixture that shifts the reaction course to lower temperature. Solid solution of $SrSn_{0.975}Cr_{0.025}O_{3-\delta}$ was prepared at temperature 1200 °C. The optimal composition for synthesis of the intense red-pink powder is $SrSn_{0.975}Cr_{0.025}O_{3-\delta}$ (L*/a*/b* = 36.34/14.21./1.12). Red-pink colour of the pigments is explained in terms of crystal field theory. The partial substitution of tin ions by chromium ions leads to formation of the optical absorption bands corresponding to the O_{2p}–Cr_{3d} charge transfer transitions. Pigment is distinguished by good chemical stability in a molten ceramic glaze and high value of solar reflectance in the near infrared region of light (R* ≈ 61%).

Key words: *Pink pigment, Perovskites, Thermal processing, TG/DTA analysis, NIR pigments*

1. Introduction

There is current interest in the ceramic industry for developing more stable pigments that present intense tonalities and which are in agreement with the technological and environmental requirements [1]. The present investigation was directed toward obtaining ceramic pigments with red-pink colour and intense tonality, which are at present difficult to obtain. Currently, there are industrial ceramic pigments with pink hues with the following structures [2]:

- Manganese alumina pink corundum (CPMA no. 3-04-5) [3,4] is the pigment exceptionally suitable for colouring clay bodies, but it is not generally used in ceramic glazes or porcelain enamels.
- Chrome alumina pink corundum (CPMA no. 3-03-5), Chrome tin orchid cassiterite (CPMA no. 11-23-5) [3], Chrome tin pink sphene (CPMA no. 12-25-5) [3,4], Chrome alumina pink spinel (CPMA no. 13-32-5) [3,4], and Zirconium iron pink zircon (CPMA no.14-44-5) [3] are the pigments exceptionally suitable for colouring ceramic glazes.
- Red $CdSe_xS_{1-x}$ encapsulated in zircon structure [5].
- Reddish-brown $Ce_{1-x}Pr_xO_2$ with fluorite structure [5].

The only pigment that presents an intense red tonality is cadmium sulfoselenide. The use of this compound is limited by its low thermal stability. It decomposes in oxidizing atmospheres at temperatures above 600 °C. Another difficulty is the high toxicity of the materials used in its manufacture [5]. The iron (III) in the zirconium iron pink zircon

pigment experiences reduction at high temperature with formation of variable contents in Fe (II), which explains the modification of the colour.

Obtaining non-toxic ceramic pigments with high temperature stability requires searching for new host structures and new synthesis methods involving less toxic materials, which must also be economically profitable [1]. According to Marinova et al. [1], these materials can be replaced by refractory oxides such as yttrium and aluminium oxide, which generally have a low toxicity rating. The yttrium and aluminium perovskite structure exhibits great thermal stability, chemical resistance, quality, and possible applications in ceramic glazes. The octahedral coordination in the perovskite structure is appropriate for introducing the Cr(III) ions, modulating this octahedral environment toward a strong crystal field, providing the red colour [6–8]. A red pigment based on perovskite structure $YAl_{1-y}Cr_yO_3$ (y = 0.01–0.1) has also been studied by Ahmadi et al. [9, 10]. Authors synthetized the pigments by co-precipitation method, and via solution combustion method, using as a mineralizer mixture of $3NaF+2MgF_2+1Li_2CO_3$. The most intense redness was obtained when y was 0.03. The results also showed that the molar ratio of the fuel to oxidizer determines the quality of the pigment in terms of colour shade [10]. The research by Martos et al. [11] was focused on the optimization of the synthesis parameters of $ZnAl_{2-x}Cr_xO_4$ spinel pigments to minimize the amount of pollutant Cr(VI) in the washing liquids and enhance chromatic coordinates. Colorimetric study and quantitative analysis of leached Cr(VI) in the washing liquids showed that the optimal composition corresponds to $ZnAl_{1.8}Cr_{0.2}O_4$. Thus, this work has enabled the production of a pink pigment with low environmental impact and good chromatic parameters.

Searching for new host structures led to the study of ceramic pink pigments based on lutetium gallium garnet doped with chromium and calcium. In the $Ca_xCr_xLu_{3-2x}Ga_5O_{12}$

(x=0.05-0.6) system, solid solutions incorporating both Cr(III) and Cr(IV) ions were obtained. Cr ions occupy basically dodecahedral sites substituting for Lu(III), and their predominant oxidation state up to x = 0.2 composition, giving a pink coloration in the ceramic glaze matrix, is Cr(IV) [12]. Role of Cr(IV) as red chromophore was described also in work regarding synthesis of $Ca(Cr_xTi_{1-x})O_3$ [13,14]. Cr(IV) and Cr(III), both in octahedral coordination, substitute Ti(IV) in the titanate lattice. Cr(IV) ions act as the red chromophore agent associated with its 520 nm absorption band in red-pink samples, but at higher x values (blue samples), Cr(III) ion affects the colour with its absorption at 600 nm. Moreover, $CaCrO_4$ crystallizes when x increases, producing green colour in glazed samples. This can be avoided using NH_4Cl as the mineralizer. García studied the effect of Mg, Ca, Sr, Ba ions on the coloration of pink inorganic pigment $M(Ti_{1-x}Cr_x)\ O_3$, where M = Mg, Ca, Sr, Ba and x = 0.003, 0.005, 0.01, 0.1 compositions [15]. Cr-$MgTiO_3$ crystallizes at magnesium ilmenite with residual $MgCr_2O_4$ spinel that inhibits the Cr entrance in solid solution and does not show pigmenting properties. Cr-$CaTiO_3$ forms orthorhombic perovskite pink solid solutions associated to Cr(IV)-Ti(IV) substitution, which is unstable in glaze above x = 0.03 and produces light green shades. Cr-$SrTiO_3$ forms ideal cubic perovskite pink solid solutions that are unstable in glaze above x=0.01. Cr-$BaTiO_3$ crystallizes in tetragonal perovskite structure with residual peaks of $BaCrO_4$ at x = 0.1 showing pink solid solution until x=0.05 that destabilizes in glazes above x = 0.03 [15]. The Cr-$SrTiO_3$ system was also prepared later by sol-gel method [16]. A secondary phase of $SrCr_2O_7$ was detected at high Cr doping.

The present research work is focused on synthesis and characterization of oxide materials based on host structure of $SrSnO_3$ doped with Cr(III) ion. In the work, the technological

effect of different methods of preparation on phase composition, optical properties and the pigment qualities were studied.

2. Experimental

2.1. Preparation of samples

The pigments $SrCr_xSn_{1-x}O_{3-\delta}$ (x = 0; 0.025; 0.05; 0.1; 0.2 and 0.3) were prepared by suspension mixing of materials (SMM), by classical ceramic method (SSR) and by mechanochemical activation (MA). The first synthesis route, called SMM, represents formation of suspensions of initial reagents and its thermal treatment in two steps [17]. These initial reagents were used for SMM synthesis route: $SrCO_3$ (96% purity, ML Chemica, CR), Cr_2O_3 (99% purity, Koltex, s.r.o., CR), SnO_2 (99% purity, Shepherd Color Company, USA), and mixture of fumaric acid (99% purity, Acros Organics, USA) and urea (99.5% purity, PLIVA - Lachema, a.s., CR) in wt. ratio 3.5:1. The first step of synthesis represents the thermal treatment of the aqueous suspension on an steel plate for 15 min; temperature ≈ 400 °C, which led to the formation of the activated intermediate. The second step of synthesis represents a classical calcination of the activated intermediate in an electric resistance furnace on air (900-1500 °C; 10 °C.min^{-1}, 3 h). The second method of the synthesis is based on the classical ceramic route, that is, solid-state reaction (SSR). The initial reagents ($SrCO_3$, SnO_2 and Cr_2O_3) were weighted in appropriate proportions (ls) and thoroughly homogenized in a mortar grinder Pulverisette 2 (Fritsch GmbH, Germany) for 15 min. Then the reaction mixtures were calcinated in an electric resistance furnace (900-1500 °C; 10 °C.min^{-1}, 3 h). The third method of preparation contains additional mechanochemical activation (MA) of homogenized initial reagents before heating. The reaction mixtures containing $SrCO_3$, SnO_2 and Cr_2O_3 were

subjected to mechanochemical activation in a planetary mill Pulverisette 5 (Fritsch GmbH, Germany) for 6 h, at a rotation speed of 200 rpm. Each reaction mixture was milled together with agate balls (ø 10 mm) in a ball-to-powder mass ratio of 20:1. Then, mechanochemically activated reaction mixtures were calcinated in an electric furnace at the temperature range 900–1500 °C for 3 h [18].

Methods of thermal analysis were used to study the differences in thermal behaviour of activated reaction mixtures by heat in the case of SMM method, and mechanochemical activation in the case of MA method, and compared to the non-activated reaction mixture (SSR). Simultaneous TG/DTA analysis of the reaction mixtures was performed by using STA 449C Jupiter (NETZSCH, Germany). Powder specimens (460–510 mg) in corundum crucibles were heated up to a temperature of 1350 °C with a heating rate of 10 °C min^{-1} in air. α-Al_2O_3 was used as a reference material.

2.2. Characterization of samples

The phase composition of the pigments was studied by X-ray diffraction analysis. The diffractograms of the samples were obtained by using a diffractometer Brucker (GB) D8 Advance (Bruker, GB) with a goniometer of 17 cm in the range 2θ of 10–80°. $CuK_{\alpha 1}$ ($\lambda = 0.15418$ nm) radiation was used for angular range of $2\theta < 35°$ and $CuK_{\alpha 2}$ ($\lambda = 0.15405$ nm) for the range of $2\theta > 35°$. A scintillation detector was used. The identification of individual phases was based on the accordance of the obtained diffraction patterns with the data contained in the PDF cards [19].

The colour qualities of the pigments were evaluated after their application to the organic matrix (dispersive acrylic paint Luxol, AkzoNobel) in mass tone and to the ceramic glaze "G-07091" (Glazura s.r.o., Roudnice nad Labem CR). The slurry containing 1 g of the

pigment and 1.5 cm^3 of the organic matrix was homogenized in an agate mortar. Coloured paints were prepared by deposition of the slurries on the white non-absorbing paper. The thickness of the wet film was 100 μm. For testing of the pigments in the ceramic glaze, aqueous suspensions containing 15 wt.% of the pigment and 85 wt.% of the glaze were prepared by hand milling. These slurries were deposited using a brush on wall tile bodies and fired for 15 min at 1000 °C.

The colour properties of all films were objectively evaluated by measuring of the spectral reflectance by using a spectrophotometer Colour Quest XE (HunterLab, USA). The measurement conditions were as follows: an Illuminant D65 and measuring geometry d/8°. For description of colour, the CIE L*a*b* colour space (also referred as CIELAB) was used [20].

The diffuse reflectance of the samples in the NIR range of light was measured by a spectrophotometer UV-3600 Plus (Shimadzu, Jpn.) with integrating sphere attachment and using $BaSO_4$ as a reference. The NIR solar reflectance (R^*) in the wavelength range of 700–2000 nm was calculated according to the ASTM G Standard 173-03. The function R^* is defined as:

$$R^* = \frac{\int_{700}^{2000} \mathrm{r}(\lambda)\,\mathrm{i}(\lambda)\,\mathrm{d}\lambda}{\int_{700}^{2000} \mathrm{i}(\lambda)\,\mathrm{d}\lambda} \qquad (1)$$

where $r(\lambda)$ is the experimentally achieved spectral reflectance from the experiment and $i(\lambda)$ is the standard solar spectrum ($Wm^{-2}mm^{-1)}$ determined from ASTM Standard G 173-03.

Particle size distribution of the samples was measured by using a Mastersizer 2000/MU (Malvern Instruments, UK). The equipment employs a scattering of incident light on particles. The signal was evaluated on the basis of Mie theory.

Scanning electron micrographs of the materials were taken with high-resolution scanning electron microscope (JOEL JSM-5500 LV (JOEL Inc. USA) to study the surface morphology and grain size of the calcined pigment powders. The accelerating voltage of the primary electron beam was 20 kV.

3. Results and discussion

3.1. Thermal analysis and XRD results

The different thermal behaviour of reaction mixtures of $SrCr_{0.025}Sn_{0.975}O_{3-\delta}$ is clearly visible from TG and DTA curves in Fig. 1 (SSR reaction mixture; 468.4 mg), Fig. 2 (MA-mechanochemically activated reaction mixture; 506 mg) and in Fig. 3 (SMM- heat activated reaction mixture; 468.6 mg). The total mass losses in the SSR mixture and the MA mixture are almost the same ≈ 15.2%, but the shape of the curves is different. The TG curve of the SSR reaction mixture (Fig. 1) contains two steps, and mass loss is completed at 1250 °C whereas the TG curve of the MA reaction mixture (Fig. 2) contains three steps, and mass weight of the sample is constant from 1190 °C. The total mass loss of the SMM reaction mixture is 16.22 % (Fig. 3, Table 1). Higher mass loss is caused by presence of the residual organic compounds (urea and its decomposition by-products) that decompose in a temperature region from 30 to 620 °C (-1.02 %) [21,22]. Mass loss of the SMM reaction mixture is completed from 1075 °C. Results of TG analysis show the effectivity of activation of reaction mixtures either mechanochemically or by heat, because it shifts the reaction course to lower temperatures.

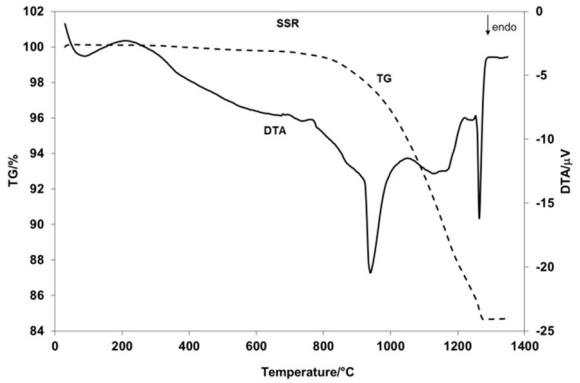

Fig. 1 Thermal analysis results of the SSR reaction mixture ($SrCO_3$, SnO_2 and Cr_2O_3)

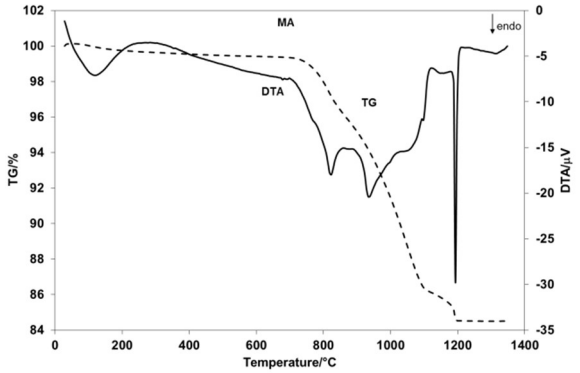

Fig. 2 Thermal analysis results of the MA reaction mixture ($SrCO_3$, SnO_2 and Cr_2O_3)

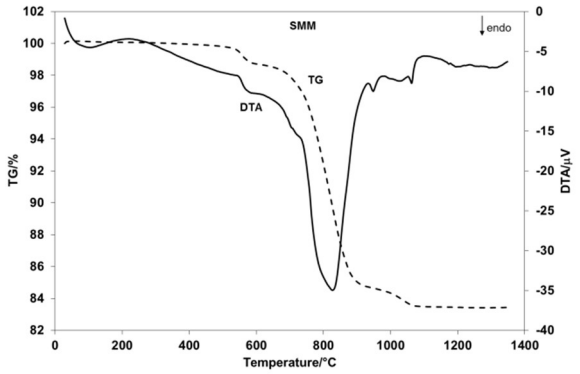

Fig. 3 Thermal analysis results of the SMM reaction mixture ($SrCO_3$, SnO_2, Cr_2O_3, urea)

In the temperature range from 30- to 1220 °C, two exothermic effects and one significant endothermic effect were detected at the DTA curve of the SSR mixture (Fig. 1, Table 1) accompanied with mass loss. Two very weak exothermic effects with maximum at 679 °C and 761 °C are associated with formation of new phases Sr_2SnO_4 and $SrSnO_3$. The

formation of $SrSnO_3$ through the intermediate Sr_2SnO_4 bellow the temperature 1000 °C was published by Berbenni [23]. The presence of Sr_2SnO_4 and $SrSnO_3$ phases were detected by the XRD analysis in the sample prepared by SSR reaction calcinated at 900 °C (Table 2). Significant endothermic peak with the minimum at 939 °C doubled with slight break at 864 °C is connected with the decomposition of $SrCO_3$. The thermal decomposition of strontium carbonate begins bellow the temperature 900 °C by crystalline transition ($\gamma \rightarrow \beta$) [24] and goes on several steps [25-27]. Thermal analysis of $SrCO_3$ studied by Ianculescu in the region 30-1100 °C presents two endothermic peaks: the first at 930 °C, and second at 1027 °C [28]. Thermal decomposition of used $SrCO_3$ in the temperature region from 30 to 1300 °C was published previously and four endothermic effects were detected at the DTA curve: two weak endothermic effects (863 °C and 1182 °C) and two sharp endothermic effects (937 °C and 1240 °C) [25]. Not all these effects are detected at the DTA curve of the SSR mixture (Fig. 1). In the temperature region from 1000 to 1250 °C, the decomposition of $SrCO_3$ continues (two slight breaks at 1130 °C and 1170 °C) and also reaction between SrO, resp. $SrCO_3$, and Cr_2O_3 takes place and therefore Sr-Cr-O compound is formed. Four stable ternary compounds, $SrCrO_4$, $Sr_3Cr_2O_8$, Sr_2CrO_4 and $SrCr_2O_4$, can be formed during reaction between $SrCO_3$ and Cr_2O_3 [29]. The presence of any Sr-Cr-O ternary compound was not proved by XRD analysis of the SSR mixture after calcination at 900 °C and 1000 °C. But the phase composition of the SSR mixture after calcination at 1100 °C and 1200 °C showed the presence of $SrCrO_4$ (Table 2). $SrCrO_4$ was prepared by Jacob and Abraham by heating mixture of $SrCO_3$ and Cr_2O_3 at 1025 °C [29]. The sharp endothermic effect with minimum at 1263 °C, which is the typical for melting of compounds, gives evidence of melting the $SrCrO_4$. Melting temperature of $SrCrO_4$ is in literature reported at 1281 °C [29]. XRD

analysis of the sample after annealing at 1300 °C detected the lines that correspond to $SrSnO_3$ type solid solution, and three lines that were not identified. The formation of $SrSnO_3$ type solid solution is completed after annealing at 1400 °C (Table 2). The $SrSnO_3$ type solid solution (1400 °C) crystallizes into cubic perovskite structure with lattice parameter a = 0.4034 nm (JPDF No. 04-008-6517) [19]

Table 1 Thermoanalytical data of the reaction mixtures SSR, MA and SMM taken from Fig. 1-3

Method	Temp. range/°C	Peak temp./°C	Mass change/%
SSR	30-1220	679 (exo); 761 (exo); 939 (endo)	-14.1
	1220-1250		-1.11
	1250-1350	1263 (endo)	—
MA	30-870	822 (endo)	-4.04
	870-1085	936 (endo)	-4.92
	1085-1190	1097 (exo)	-6.47
	1190-1350	1194 (endo)	—
SMM	30-640	542 (exo)	-1.02
	640-975	730(exo); 826 (endo); 947 (endo)	-14.06
	975-1350	1062 (endo)	-1.14
	1075-1350	—	—

The DTA curve of the mechanochemically activated MA reaction mixture is shown in Fig. 2. The different shape of the DTA curve in comparison with Fig. 1 indicates the positive effect of the activation on the reactivity of the mixture. On the DTA curve, there are two endothermic effects (822 °C and 936 °C) accompanied by slight break at 736 °C that are connected with the decomposition of $SrCO_3$ [25-27]. The exothermic effects which inform about crystallization of Sr_2SnO_4 and $SrSnO_3$ are missing at the DTA curve

(Fig. 2), but the XRD analysis of the MA mixture after calcination at 1000 °C detected the presence of $SrSnO_3$ perovskite phase and absent of Sr_2SnO_4 (Table 2). The same result brought the synthesis of $SrSnO_3$ from strontium oxalate and tin oxide [23]. Direct solid state reaction of strontium oxalate and tin oxide led to formation of $SrSnO_3$ through Sr_2SnO_4, but the mechanothermally activated solid state reaction led to formation of $SrSnO_3$ without previous formation of Sr_2SnO_4 [23]. Formation of $SrCrO_4$ is detected at the DTA curve by slight exothermic effect at 1097 °C and its melting is recorded by sharp endothermic effect at 1194 °C. Mechanochemical activation supports the formation of $SrSnO_3$ type solid solution at lower temperature; the reaction is completed after annealing at 1200 °C (Table 2). The $SrSnO_3$ type solid solution (1200 °C) crystallizes into cubic perovskite structure with lattice parameter a = 0.40363 nm (JPDF No. 04-008-6517) [19]. Thermal behaviour of the SMM reaction mixture is shown in Fig. 3. The first exothermic peak with the maximum at 542 °C is related with thermal decomposition of the foaming agents, that is, urea and its decomposition by-products [21,22]. This effect is connected with mass loss of 1.02 % at the TG curve. Very weak exothermic effect with maximum at 730 °C is related to $SrSnO_3$ formation. Increasing temperature brought three endothermic effects at the DTA curve with minimum at 826, 947, and 1062 °C, which are related to the transformation and decomposition of $SrCO_3$ [25-27]. At the temperature 1200 °C the decomposition of $SrCO_3$ is finished and powder is composed from three phases: $SrSnO_3$, SnO_2 and one no identified phase. In the temperature range from 1200 to 1300 °C are evident weak waves on the DTA curve, but any effect was not detected; although, formation of pure $SrSnO_3$ type solid solution was proved by the XRD analysis in that region (Table 2). The lack of sharp endothermic effect in the temperature range from 1150 to 1350 ° C, which would be responsible for melting of $SrCrO_4$, indicates that

$SrCrO_4$ is not reaction product. Results of TG/DTA analysis showed that SMM method allows the synthesis of Cr-doped $SrSnO_3$ pigments without formation of $SrCrO_4$, and therefore, from the technological and environmental point of view, the SMM method seems to be the suitable for synthesis of this type of perovskite pigments. However, single-phased solid solution of the $SrSnO_3$ type can be prepared by MA method and by anealing at temperature of 100 °C lower.

Table 2 The effect of synthesis route on phase composition of powder $SrCr_{0.025}Sn_{0.975}O_{3-\delta}$

Method of preparation	Crystalline phases
SSR, 900 °C	SnO_2, $SrCO_3$, Sr_2SnO_4, $SrSnO_3$, Cr_2O_3
SSR, 1000 °C	SnO_2, $SrSnO_3$, Sr_2SnO_4, $SrCO_3$, SrO, Cr_2O_3
SSR, 1100°°C	SnO_2, $SrSnO_3$, Sr_2SnO_4, $SrCO_3$, SrO, Cr_2O_3, $SrCrO_4$
SSR, 1200 °C	$SrSnO_3$, SnO_2, Sr_2SnO_4, $SrCO_3$, Cr_2O_3, $SrCrO_4$
SSR, 1300 °C	$SrSnO_3$; unidentified phase
SSR, 1400 °C	$SrSnO_3$ type solid solution
MA, 1000 °C	$SrSnO_3$, SnO_2, $SrCO_3$, Cr_2O_3
MA, 1200 °C –1400 °C	$SrSnO_3$ type solid solution
SMM, 1200 °C	$SrSnO_3$, SnO_2, unidentified phase
SMM, 1300 °C – 1400 °C	$SrSnO_3$ type solid solution

The effect of increasing amount of Cr(III) ions added to the host lattice of $SrSnO_3$ (SMM; 1300 °C) on the phase composition of powders is shown in Fig. 4. An amount of Cr(III) higher than 0.05 caused formation of secondary phase. Its crystalization is clearly visible in left inset of Fig. 4 (2θ = 27.29 °). The synthesis route did not eliminate the formation of secondary phase in the range of substitution x=0.05-0.3. The diffraction intensity of

perovskite phase decreases with increase of dopant concentration (given in the right inset of Fig. 4), which indicates that the Cr dopant affects the growth mechanism of perovskite phase. Similar results regarding the crystallization of $SrSnO_3$ doped by Cr ions were observed in the work of Muralidharan et al. [30].

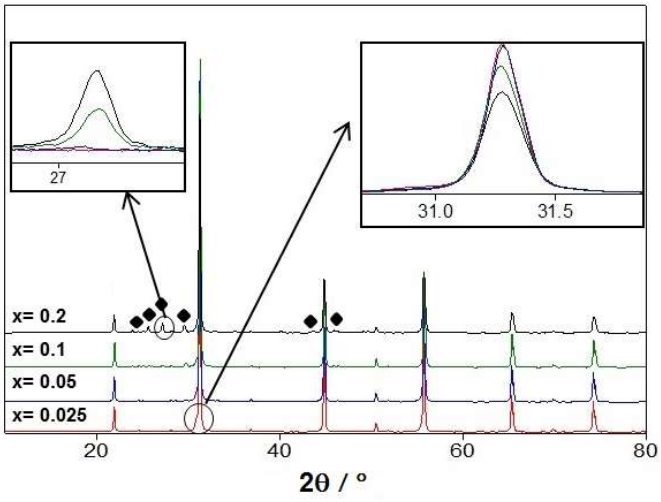

Fig. 4 XRD of samples $SrCr_xSn_{1-x}O_{3-\delta}$ prepared by SMM method by heating at 1300 °C (♦unidentified diffraction line).

3.2. Particle size distribution

The preparation method and the heating temperature can significantly affect the particle size distribution (PSD) and thus the colour properties. The first PSD measurement of samples calcined at 1300 °C was made after preliminary grinding in an agate mortar. Samples of pigments that were prepared by the SSR method and by the SMM method are characterized by mean values in the interval of d_{50} from 3.5 μm to 4.8 μm. However, the mean value of the pigment particles that were prepared by MA method is only 2.03 μm (Table 3). Although, the values of mean between 2μm and 5 μm seem to be optimal for utilization of pigments for colouring of ceramic glaze, the wide range of the particle size distribution indicates the necessity to reduce the particle size. In the SSR method, a better

granulometric composition was obtained after 10 min of wet milling, but the optimal particle size distribution of all samples was obtained after 20 min of milling in planetary mill in ethanol and zircon balls (ø 1 mm) (250 rps) (Table 3).

Table 3 The effect of milling on the values of particle size of pigments $SrCr_{0.025}Sn_{0.975}O_{3-\delta}$ (1300 °C)

Wet milling /min	SSR		MA		SMM	
	d_{10}-d_{90}/μm	d_{50}/μm	d_{10}-d_{90}/μm	d_{90}/μm	d_{10}-d_{90}/μm	d_{90}/μm
0	0.90-18.61	4.75	0.44-13.56	2.03	0.55-13.26	3.70
10	0.66-13.47	3.60	0.42-11.09	1.95	0.52-13.17	3.18
20	0.60-10.78	3.14	0.41-9.44	1.79	0.48-11.07	2.76

Electron microscopy was used to characterize the perovskite pigments with respect to their overall appearance and to confirm the results of the PSD measured by laser diffraction. Fig. 5a and Fig. 5b demonstrate the similar, almost spherical, shapes of particles prepared by the SSR and SMM methods. Particles in the powders are predominantly of the size 1 μm. The particles prepared by the MA method are smaller than those from the SSR and SMM methods (Fig. 5c). This result might explain the divergence in the colour properties of the samples prepared by the MA method.

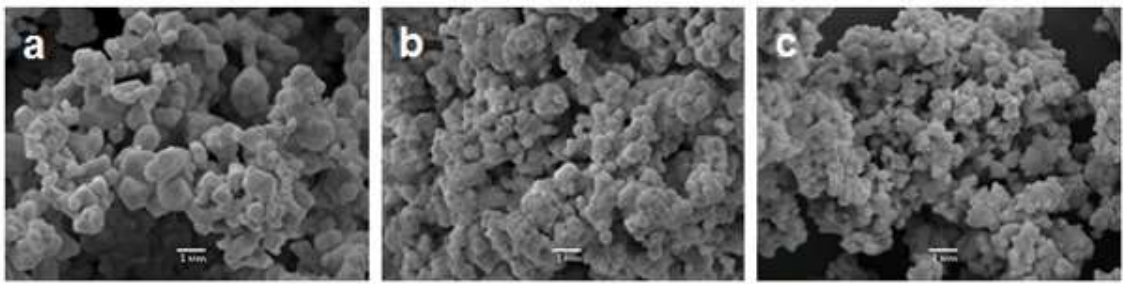

Fig. 5 SEM images of pigment $SrCr_{0.025}Sn_{0.975}O_{3-\delta}$ prepared by: (a) the SSR method; (b) the SMM method and (c) the MA method obtained upon calcination at 1300°C (magnification x10000)

*3.3. Measurement of colour in the CIE L*a*b* system*

The colour qualities of all pigments were evaluated after 20 min of wet milling. The effect of calcining temperature and the method of preparation on the colour parameters of the pigment $SrCr_{0.025}Sn_{0.975}O_{3-\delta}$ applied to an organic matrix in mass tone are summarized in Table 4. All methods of preparation are associated with the darkening of the pigment (↓ *L**) due to the increasing calcining temperature. At the same time, a change in the colour shade can be observed for all the methods. The increasing calcination temperature from 1300 °C to 1500 °C reduces the amount of red (+*a**) and yellow (+*b**) hue. While the samples prepared at 1300 °C are pink-violet, raising the temperature promotes the formation of red-pink (1400 °C) to pure brown hue (1500 °C). The effect of the preparation method on pigment colouring is more evident at lower calcination temperatures (1300 and 1400 °C), which is probably associated with the phase composition of the samples. The heating temperature of 1500 °C gives rise to powders of comparable colour properties. From colour point of view, the most interesting pigment was prepared by the SSR method with calcination at 1400 °C. This powder has red-pink colour with the highest chroma.

Table 4 The effect of the synthesis route on the colour parameters of $SrCr_{0.025}Sn_{0.975}O_{3-\delta}$ powder applied into organic matrix.

T/°C	SSR			MA			SMM		
	L*	a*	b*	L*	a*	b*	L*	a*	b*

1300	42.55	18.61	2.16	43.82	18.06	3.16	40.87	17.34	4.26
1400	36.34	14.21	1.12	35.75	12.47	0.59	38.31	16.18	3.11
1500	34.42	12.39	1.05	34.68	10.29	0.46	31.99	10.02	0.87

The colour parameters of the powders $SrCr_{0.025}Sn_{0.975}O_{3-\delta}$ were also evaluated after they were applied in the ceramic glaze (Table 5). In terms of colour, the pigments prepared by the SSR and SMM method are comparable; after application on the ceramic glaze, both provide dark red-pink surface that is colour homogenous and produces a smooth, glossy surface on a ceramic substrate. From the point of view of the quality of the pigment application, it can be stated that the pigment prepared by the SSR method and heated at 1400 ° C is the most suitable for application to the ceramic glaze as it does not contain any surface defects. Pigments prepared by the MA method provide brownish colour in the ceramic glaze, especially at higher firing temperatures (1400 and 1500 °C) and, moreover, they do not colour the surface of the ceramic substrate uniformly. As in the case of colouring organic matrix, in all methods of preparation the increase of heating temperature causes the darkening of the pigment application.

Table 5 The effect of the synthesis route on the colour parameters of $SrCr_{0.025}Sn_{0.975}O_{3-\delta}$ powder applied to ceramic glaze.

T/°C	SSR			MA			SMM		
	L*	a*	b*	L*	a*	b*	L*	a*	b*
1300	51.68	14.70	4.86	50.28	14.99	6.61	49.01	14.00	6.14
1400	48.24	14.54	4.59	49.53	15.29	9.49	48.04	14.72	5.13
1500	47.09	15.54	5.43	45.90	14.31	7.50	45.71	14.62	5.01

3.4. UV–VIS–NIR spectroscopy

Usually the colour of the Cr-doped inorganic pigments is explained according to the crystal field theory applied to Cr(III). It has d^3 electronic configuration, and in mixed oxides prefers octahedral coordination. Several electronic transitions are possible in this case [31]. The most intense transitions $^4A_{2g}$ (^4F) → $^4T_{2g}$ (^4F) (U-band) and $^4A_{2g}$(^4F) → $^4T_{1g}$ (^4F) (Y-band) are in the visible part of light. The third intense transition $^4A_{2g}$ (^4F) → $^2T_{1g}$ (^4P) (Y'-band) is usually centred in a high UV range. In addition, the transitions corresponding the $^4A_{2g}$ (^4F) → ^2E_g (^2G) (R- band) and $^4A_{2g}$ (^4F) → $^2T_{1g}$ (^2G) (R'-band) are also observed in a visible range of light, although less intense than Y and U bands [32]. Fig. 6 shows the optical absorption spectra of $SrCr_{0.025}Sn_{0.975}O_{3-\delta}$ (SSR; 1400 °C) and Cr_2O_3 (Koltex, s.r.o., CR) applied to the ceramic glaze measured in diffuse reflectance mode in the UV–VIS spectral range. The absorption spectrum of Cr_2O_3 is dominated by three intense bands: 378 nm (Y'-band), 463 nm (Y-band) and 602 nm (U-band). Additionally, the weak peak around 714 nm is associated with R, R' bands forbidden by both spin selection and Laporte's rules. The red-pink glazed tile with $SrCr_{0.025}Sn_{0.975}O_{3-\delta}$ (SSR; 1400 °C) shows two transfer bands at the absorption spectrum in Fig. 6. The first one is centred at 363 nm and the second, broad absorption band is centred at 542 nm. These bands can be explained by the formalism of the crystal field theory applied to Cr(IV) in octahedral coordination, with its characteristics bands, namely, $^3A_{2g}(F) \rightarrow {}^3T_{1g}(P)$ (363 nm) and $^3A_{2g}(F) \rightarrow {}^3T_{1g}(F)$ (542 nm) [13].

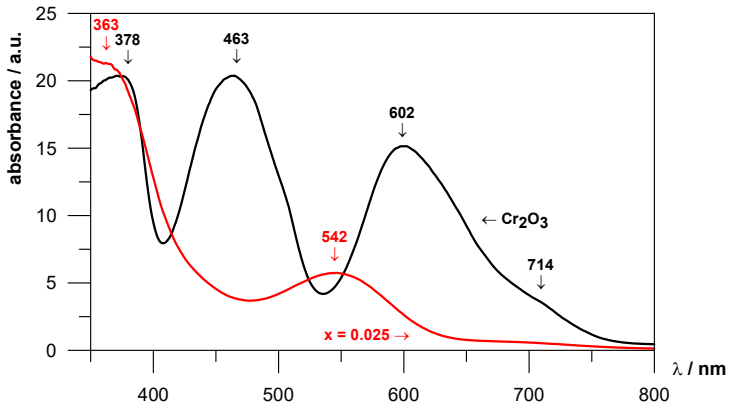

Fig. 6 Absorption spectra of the $SrCr_{0.025}Sn_{0.975}O_{3-\delta}$ (SSR; 1400 °C) and Cr_2O_3 applied to the ceramic glaze.

The UV–VIS spectrum of khaki glazed tile with $SrCr_{0.3}Sn_{0.7}O_{3-\delta}$ (SSR; 1300 °C) is given in Fig. 7. The broad absorption band can be decomposed in four weak bands centred at 370 nm, 461 nm, 598 nm, and 700 nm. All these bands correspond to electronic transitions of Cr(III) in octahedral coordination. The absorption bands of the pigment with increase of substitution of Sn ions by Cr ions are very weak due to coexistence of electronic transitions of Cr(III) and also Cr(IV). Characteristic band of Cr(IV) centred in the VIS region around 520–550 nm is overlapped by Y-band and U-band of Cr(III) centred at 460 nm and 598 nm.

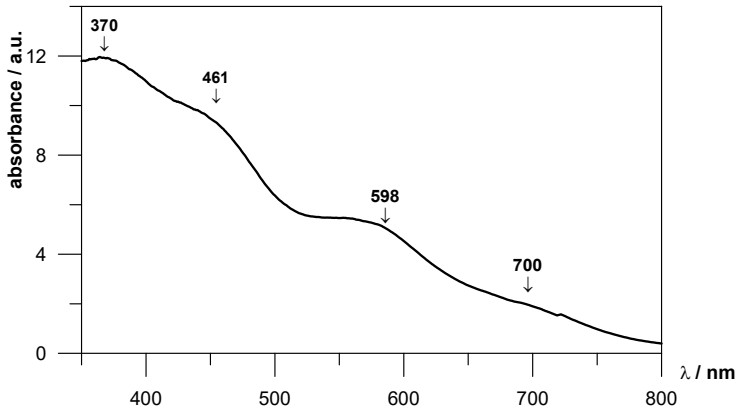

Fig. 7 Absorption spectrum of the $SrCr_{0.3}Sn_{0.7}O_{3-\delta}$ (SSR; 1400 °C) applied to the ceramic glaze.

Infrared radiation incident on objects generates heat, and absorption in the range of 700 to 1100 nm leads to significant surface heating. This is the reason why infrared reflective pigments are increasingly used for colouring of roofs and building materials [33]. The infrared reflective inorganic pigments are colour pigments, which reflect the wavelengths in infrared region in addition to reflecting some visible light selectively [34]. In order to assess utilization of the pigments as functional materials intended for colouring of buildings materials, the NIR reflectance spectra of the pigments were measured and also calculated their NIR solar reflectance spectra in the range 700–2000 nm (Fig. 8). The values of NIR reflectance (R) and solar reflectance (R^*) of the pigments $SrCr_xSn_{1-x}O_{3-\delta}$ (SSR; 1400 °C) applied to the ceramic glaze are given in Table 6. Their values of NIR solar reflectance (R^*) are in a range 61.32–48.64 %. Increasing amount of chromium ions added into the perovskite structure decreases the R^* values. All perovskite samples $SrCr_xSn_{1-x}O_{3-\delta}$ have values of (R^*) higher than 20%, and therefore they can be called "cool pigments" and can be recommended for colouring of building materials, where they have energy-saving potential.

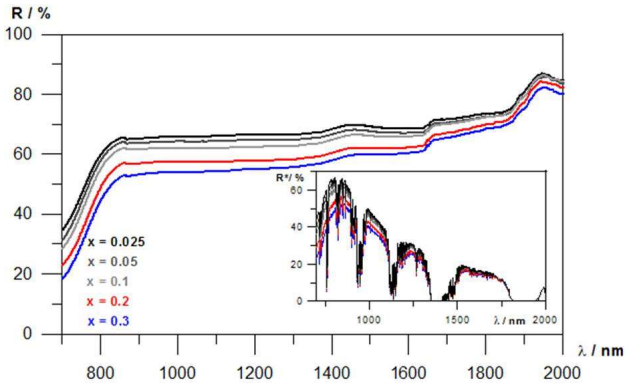

Fig. 8 NIR reflectance and NIR solar reflectance spectra of $SrCr_xSn_{1-x}O_{3-\delta}$ (SSR; 1400 °C) applied to ceramic glaze.

Table 6 The values of NIR reflectance (R) and solar reflectance (R^*) of the pigments $SrCr_xSn_{1-x}O_{3-\delta}$ (SSR; 1400 °C) applied to the ceramic glaze

	x=0.025	x=0.05	x=0.1	x=0.2	x=0.3
$R_{(700-2000)}$/ %	65.69	64.00	62.13	57.66	54.77
$R^*_{(700-2000)}$/ %	61.32	59.43	57.15	52.11	48.64

4. Conclusion

From the above discussion, following conclusions can be summarized:

- The pigments were synthesized by the conventional ceramic method (SSR), suspension mixing of materials (SMM), and by the mechanochemical activation (MA) of initial reagents in the temperature range 1000–1500 °C. Results of TG/DTA and XRD analysis showed that the mechanochemical activation of initial reagents allows the synthesis of $SrSn_{0.975}Cr_{0.025}O_{3-\delta}$ powder at the lowest temperature (1200 °C). Therefore, from the technological and environmental point of view, the mechanochemical activation method is the most suitable method of synthesis.

- Pigments of the general formula $SrCr_xSn_{1-x}O_{3-\delta}$, where x = 0.025, 0.05, 0.1, 0.2 and 0.3, have deep red-pink to reddish-brown colour hues. The optimal composition for preparation of the intense red-pink powder is $SrSn_{0.975}Cr_{0.025}O_{3-\delta}$. From colour point of view, the most interesting pigment was prepared by the SSR method with calcination at 1400 °C.

- Colour of the pigments is explained in terms of crystal field theory. The partial substitution of tin ions by chromium ions in amount of x = 0.025 leads to formation of the optical absorption bands corresponding to the O_{2p}–Cr_{3d} charge transfer transitions. These bands with maximum at 370 and 540 nm correspond to the transitions of electronic

configuration of Cr(IV). Higher amount of Cr ions than $x = 0.05$ added to $SrCr_xSn_{1-x}O_{3-\delta}$ powders caused formation of secondary phase.

- The $SrSn_{0.975}Cr_{0.025}O_{3-\delta}$ pigment exhibits high NIR solar reflectivity and can be classified as “cool pigment”.

Acknowledgements

This work has been supported by Grant Agency of Czech Republic, project No. 16-06697S.

The authors thank the Center of Materials and Nanotechnologies (CEMNAT) for providing UV-VIS-NIR spectroscopy.

References

1. Marinova Y, Hohemberger JM, Cordoncillo E, Escribano P, Carda JB. Study of solid solutions with perovskite structure for application in the field of the ceramic pigments. J Eur Ceram Soc. 2003;23:213-20.
2. Emiliani GP, Gorbara F. Tecnologia Ceramica, La lavorazione, Le tipologie. Faenza Gruppo Editoriale. 1999.
3. DCMA Clasification and Chemical Description of the Mixed Metal Oxide Inorganic Colored Pigments. Metal Oxides and Ceramic Colors Subcommitee. 2nd ed. Washington: Dry Color Manufacturer’s Assn. 1982.
4. Stefani R, Longo E, Escribano P, Cordoncillo E, Carda JB. Developing a pink pigment for glases. Am Ceram Soc Bull. 1997;76:61-4.
5. Ma Rincon J, Carda J, Alarcón J. Nuevos productos y tecnologías de esmaltes y pigmentos cerámicos. Castellón: Faenza Editrice Ibérica. 1992.

6. Alarcón J, Glasser FP. Yttrium aluminate garnets doped with chromium manganese and vanadium. J Mater Sci Let. 1988;7:187-90.

7. Chiang YM, Birnie D, Kingery WD. Physical Ceramics, Principles for Ceramic Science and Engineering. New York: John Wiley & Sons. 1997.

8. Nassau K. The Physics and Chemistry of Color: The Fifteen Causes of Color, New York: John Wiley & Sons. 1983.

9. Ahmadi S, Aghaei A, Yekta BE. Synthesis of Y(Al,Cr) O_3 red pigments by co-precipitation method and their interactions with glazes. Ceram Int. 2009;35:3485-8.

10. Ahmadi S, Aghaei A, Yekta BE. Effective parameters for synthesis of chromium doped $YAlO_3$ red pigment. Pigm Resin Technol. 2015;44:1-6.

11. Martos M, Martínez M, Cordoncillo E, Escribano P. J Eur Ceram Soc 2007;27:4561-7.

12. Galindo R, Llusar M, Tena MA, Monrós G, Badenes JA. New pink ceramic pigment based on chromium (IV) –doped lutetium gallium garnet. J Eur Ceram Soc. 2007;27:199-205.

13. Gargori C, Galindo R, Llusar M, Cerro S, Garcia A, Monrós G. New chomium-calcium titanate red ceramic pigment. Adv Sci Technol. 2010;68:208-12.

14. Gargori C, Cerro S, Galindo R, García A, Llusar M, Badenes J, Monrós G. Iron and chromium doped perovskite ($CaMO_3$ M=Ti, Zr) ceramic pigments, effect of mineralizer. Ceram Int. 2012;38:4453-60.

15. García A, Galindo R, Gargori C, Cerro S, Llusar M, Monrós G. Ceramic pigments based on chromium doped alkaline earth titanates. Ceram Int. 2013;39:4125-32.

16. Yongvanich N, Srithong K, Kaewbudsa W, Visuttipitukul P. New Cr-doped $SrTiO_3$ ceramic color pigments. Appl Mech Mater. 2015;709:346-9.

17. Mesíková Ž, Trojan M, Šulcová P. Conditions of Synthesis of Co-Zn-Ti-Cr spinel Pigment. Ceram Silik. 2005;49:28-32.

18. Adolfová L, Dohnalová Ž, Šulcová P, Matušková M. Ceramic pigments based on doped strontium stannates. J Therm Anal Calorim. 2014;116:709-14.

19. Joint Committee on Powder Diffraction Standards. International Centre of Diffraction Data. Swarthmore. JPDF. 1983.

20. Commission Internationale de l'Eclairage. Recommendations on uniform colour spaces, colour difference equations, psychometric colopur terms, supplement no. 2 of CIE publication no. 15 (E1-1.31) 1971. Paris: Bureau Central de la CIE, 1978.

21 Schaber PM, Colson J, Higgins S, Thielen D, Anspach B, Brauer J. Thermal decomposition (pyrolysis) of urea in an open reaction vessel. Thermochim. Acta 2004;424:131-42.

22. Bernhard AM, Peitz D, Elsener M, Wokaun A, Kröcher O. Hydrolysis and thermolysis of urea and its decomposition byproducts biuret, cyanuric acid and melamine over anatase TiO_2. Appl Catal B- Environ. 2012;115:129-37.

23. Berbeni Z, Milanese Ch, Bruni G, Girella A, Marini A. Mechanothermal synthesis of $SrSnO_3$. Z Naturforsch B. 2014;69:313-20.

24. Earnest ChM, Miller ET. An assessment of barium and strontium carbonates as temperature and enthalpy standards. J Therm Anal Calorim. 2017;130:2277-82.

25. Mesíková Ž, Šulcová P, Trojan M. Synthesis and description of $SrSn_{0.6}Ln_{0.4}O_3$ perovskite pigments, J. Therm Anal Calorim. 2008;9:163-6.

26. Liptay G. Atlas of thermoanalytical curves. Budapest: Akadémiai Kiadó. 1971.

27. Gallagher PK, Sanders JP, Woodward PM, Lokuhewa IN. Reaction within the system $2SrCO_3$-Fe_2O_3. J Therm Anal Calorim 2005;80:217-23.

28. Iancukescu A, Brăileanu A, zaharescu M, Guillemet I, Madarász J, Pokol G. Formation and properties of some Nb-doped $SrTiO_3$-based solid solution. J Therm Anal Calorim. 2003;72:173-80.

29. Jacob KT, Abraham KP. Phase relations in the system Sr-Cr-O and thermodynamic properties of $SrCrO_4$ and $Sr_3Cr_2O_8$. J Phase Equilib. 2000;21:46-53.

30 Muralidharan M, Anbarasu V, Elaya Perumal A, Sivakumar K. Room temperature ferromanetism in Cr doped $SrSnO_3$ perovskite system. J Mater Sci. 2017;28:4125-37.

31. Pavlov RS, Marzá VB, Carda JB. Electronic absorption spectroscopy and colour of chromium-doped solids. J Mater. Chem. 2002;12:2825-32.

32. Gorodylova N, Kosinová V, Šulcová P. Interrelations between composition, structure, thermal stability, and chromatic characteristics of new NASICON-related solid solutions of $Li_{1+x}Cr_xZr_{2-x}(PO_4)_3$. Ceram Int. 2017;43:14629-35.

33. Bendiganavale AK, Malshe VC. Infrared Reflective Inorganic Pigments. Rec Pat Chem Engineer. 2008;1:67-79.

34. Raj AKV, Prabhakar Rao P, Divya S, Ajuthara TR. Terbium doped Sr_2MO_4 [M=Sn and Zr] yellow pigments with high infrared reflectance for energy saving applications. Powder Technol. 2017;311:52-8.

List of Figures:

List of Tables: